Reflected PP arrival in anelastic media

P.F. Daley and E.S. Krebes

ABSTRACT

A homogeneous wave incident on an interface between two anelastic halfspaces in welded contact is considered. In the anelastic sense, a homogeneous wave is defined by the condition that the propagation and attenuation vectors are collinear. It has been indicated in a number of papers over the past several decades that the proper definition of the real and imaginary parts of the vertical components of the slowness vector in the reflection coefficients are not obvious for some distributions of the quality factor, Q. This can result in anomalous behaviours of both or either of the amplitude and phase of the PP reflection coefficient when displayed versus the incident propagation angle or equivalently the real part of the horizontal component of the incident slowness vector.

In an earlier work (Krebes and Daley, 2007) the question of anomalies in the amplitude and phase of the PP plane wave reflection coefficient for these distributions of the quality factor Q in adjacent anelastic halfspaces was discussed in considerable detail. In what follows, the above paper (Paper 1) will be referred to often to minimize repetition of previous discussions.

The problem of the PP reflection coefficient is addressed again here. This is done within the context of two selected approximate methods, of varying complexity, which produce acceptable behaviour for the anomalous quantities, from a numerical viewpoint. What causes this behaviour in the PP reflection coefficient may be attributed, at least in part, to improper signs being assigned to the real and imaginary parts of the radical defining the transmitted $P-$wave vertical slowness vector component. However, this may be looked upon as a symptom rather than the actual cause of the problem.

Consideration of the PP plane wave reflection coefficient is the first matter dealt with and the discussion is then extended to the high frequency geometrical optics solution of a Sommerfeld type integral, using zero order saddle point methods for determining the particle displacement vector of the reflected PP disturbance due to a $P-$wave point source incident at an interface separating two anelastic media.

One approximation of the saddle point method was presented in detail in Paper 1 and another approximate approach was suggested and is expanded on here. The accuracy of approximations to the saddle point method are established through comparison with an "exact" (numerical integration) solution.

INTRODUCTION

A recent paper in the geophysical literature (Krebes and Daley, 2007, (Paper 1)) contains a fairly detailed discussion related to the problem of the anomalous behaviour of the PP particle displacement reflection coefficient[1] at an interface separating two anelastic media, together with a survey of the relevant literature published over the past several decades by a number of authors. As this was presented in Paper 1 interested readers are referred there for a fairly thorough introduction to this topic. One of the

[1] In what follows, the "PP particle displacement reflection coefficient" will be referred to simply as the "PP reflection coefficient" as it is this quantity that is used throughout this work.

objectives of this work is to determine what is required, from a high frequency (geometrical optics) solution perspective, to produce acceptable accuracy in numerical modeling techniques. As the saddle point method is computationally fast, when compared to more "exact" solutions, it is the leading candidate for use in obtaining insight into problems related to wave propagation in geological structures displaying anelasticity.

It has been established that for PP reflection the quantity causing the anomalous behaviour is the vertical component of the slowness vector associated with the transmitted P wavefront. This parameter appears as a radical in the PP reflection coefficient but does not appear in an exponential term in the Sommerfeld type integral, so it is not included in the computation of the saddle point

The problem mentioned above occurs in an expected region, where the saddle point is near a branch point. (However, there is no indication that the total range of incidence is not affected in some manner.) The zero order saddle point method is not valid in this region as the reflected PP geometrical optics solution here should be in terms of a higher order saddle point method approximation. For that reason, a modification of the saddle point approximation will be pursued, whose major effect is (seen most clearly but not necessarily) limited to this region. The intent is to obtain numerical results that are in reasonable agreement with a numerical integration solution, at least in the pre-critical region. In the post-critical region the solution is required to be consistent with what would be seen in a similar type of problem for the elastic case. A numerically correct remedy is sought for the anomalous behaviour, which may not be theoretically rigorous.

In Paper 1, the topic of the plane wave SH reflection and transmission coefficients at an interface separating two anelastic media was discussed, as well as the PP reflection coefficient at a similar boundary type. Only the PP reflection problem will be considered here. It was determined that the anomalous case occurred where $Q_{P_1} < Q_{P_2}$ (1 – upper or incident halfspace, 2 – lower or halfspace of transmission) and that adjustments to the formal mathematical saddle point solution were required to be introduced to ensure physically realistic results. The plane wave PP reflection coefficient will be given a cursory review and, apart from plane wave dissimilarities between the two approximate methods considered, saddle point solutions will be compared with an "exact" numerical integration approach. One of these, a major topic of Paper 1, will be commented on here together with the standard saddle point method, for which it has been shown in Paper 1 that an additional assumption must be made at the reflection coefficient stage to avoid erroneous results. This results in the introduction of a modification, which forces the reflection coefficient to display a behaviour that could be considered consistent with the elastic case, and will be discussed in more detail in a later section.

Each of the anelastic halfspaces (1 – upper, 2 – lower) are parametrically defined by a real P wave velocity, V_P, a real S wave velocity, V_S, a density, ρ, and two quality factors related to P and S modes of wave propagation, Q_P and Q_S. The complex P and S velocities may be defined in terms of Q, where Q may or may not be a function of frequency, as $1/v^2 = \left(1/V^2\right)\left(1 + i/Q\right)$. Here v are the complex velocities, $v = \alpha : \left[P - Compressional\right]$ or $v = \beta : \left[S - Shear\right]$. In slowness space, the following

quantities are required: $p_1 = \alpha_1^{-1}$, $p_2 = \alpha_2^{-1}$, $p_3 = \beta_1^{-1}$ and $p_4 = \beta_2^{-1}$, with "1" referring to the upper halfspace and "2", the lower. It should be made clear that the discussion presented here is under the assumptions that $Q_{P_2} > Q_{P_1}$ with $Q_{P_1} \gg 1$ and $Q_{P_2} \gg 1$. The quantities Q_{S_1} and Q_{S_2} are both chosen to be greater than Q_{P_1}. The method of implementing a frequency dependent Q is taken from the papers of Futterman (1962) and Azimi et al. (1968). This variation will be used in the computation of synthetic traces, and will be formally introduced as later.

SADDLE POINT METHOD THEORY

Consider an interface between two anelastic halfspaces where $z = 0$ defines the interface with the z axis chosen to be positive downwards. A $P-$wave point source is located at $r = 0$ at a distance $-z_0$ above the interface in a cylindrical coordinate system and a receiver is similarly positioned at $-z$ above the interface at an offset of r. Thus, both the source and receiver are located in the upper (1) halfspace, separated by a horizontal distance of r. The lower halfspace is designated as (2). The reflected PP potential from the interface may be written as

$$\phi(r,z,\omega) = \left[\frac{i\omega}{4\pi\rho_1\alpha_1^2}\right] F(\omega) \int_0^\infty PP(p) J_0(\omega p r) \frac{p}{\xi_1} \exp\left[i\omega \hat{T}(p)\right] dp \qquad (1)$$

Aki and Richards (1980, 2002) or equivalently as

$$\phi(r,z,\omega) = \left[\frac{i\omega}{4\pi\rho_1\alpha_1^2}\right] \frac{F(\omega)}{2} \int_{-\infty}^\infty PP(p) H_0^{(1)}(\omega p r) \frac{p}{\xi_1} \exp\left[i\omega \hat{T}(p)\right] dp \qquad (2)$$

(Abramowitz and Stegun , 1980), where $F(\omega)$ is the Fourier time transform of what will assumed to be a band limited source wavelet, indicated as $f(t)$ in the time domain. $J_0(\zeta)$ is the Bessel function of zero order, $H_0^{(1)}(\zeta)$ is the Hankel function of type one and order zero, $PP(p)$ is the PP reflection coefficient at an interface between two anelastic solids (Aki and Richards, 1980, 2002) and

$$\hat{T}(p) = \xi_1 |z + z_0| . \qquad (3)$$

The radicals ξ_j and η_j are the vertical components of the slowness vector, and may be defined in terms of the complex velocities α_j and β_j (or alternatively in terms of the related points, p_j, in the complex $p-$plane) and the integration variable p, the generally complex horizontal component of the slowness vector, as

$$\xi_j = \left(\alpha_j^{-2} - p^2\right)^{1/2} = \left(p_j^2 - p^2\right)^{1/2} \quad (j = 1,2) \qquad (4)$$

and

$$\eta_j = \left(\beta_j^{-2} - p^2\right)^{1/2} = \left(p_{j+2}^2 - p^2\right)^{1/2} \quad (j = 1,2). \tag{5}$$

The radicals η_j $(j = 1,2)$ appear only in the reflection coefficient $PP(p)$, as does ξ_2.

The horizontal and vertical components of the particle displacement vector may be obtained from the reflected PP potential, equation (1), using the formula (Aki and Richards, 1980, 2002)

$$\mathbf{u} = (u_r, u_z) = \left(\frac{\partial \phi}{\partial r}, \frac{\partial \phi}{\partial z}\right) \tag{6}$$

which leads to the integral expressions

$$u_r(r,z,\omega) = \frac{\partial \phi(r,z,\omega)}{\partial r} = \left[\frac{-i\omega^2 F(\omega)}{4\pi\rho_1\alpha_1^2}\right]\int_0^\infty PP(p) J_1(\omega p r)\ \exp\left[i\omega\hat{T}(p)\right]\frac{p^2}{\xi_1}dp \tag{7}$$

$$u_z(r,z,\omega) = \frac{\partial \phi(r,z,\omega)}{\partial z} = \left[\frac{-\omega^2 F(\omega)}{4\pi\rho_1\alpha_1^2}\right]\int_0^\infty PP(p) J_0(\omega p r)\ \exp\left[i\omega\hat{T}(p)\right] p\,dp \quad . \tag{8}$$

Equivalent expressions in terms of Hankel function of type one and orders zero and one follow from equation (2).

Only the vertical component of reflected PP particle displacement will be dealt with here as the horizontal component is similar. After introducing the zero order Hankel function $H_0^{(1)}(\omega p r)$, as in equation (2), and retaining just the first term in its asymptotic expansion for large argument, the high frequency or geometrical optics formula for the vertical component of reflected PP particle displacement (equation (8)) may be written as

$$u_z(r,z,\omega) = \left[\frac{-\omega^{3/2}}{4\pi\rho_1\alpha_1^2}\right]\frac{F(\omega)e^{-i\pi/4}}{\sqrt{2\pi r}}\int_{-\infty}^{\infty} PP(p)\ \exp\left[i\omega T(p)\right] p^{1/2}dp \tag{9}$$

where

$$T(p) = pr + \xi_1 |z + z_0| . \tag{10}$$

The saddle point, p_s is given by the solution of

$$\left.\frac{dT(p)}{dp}\right|_{p=p_s} = \left. r - \frac{p|z+z_0|}{\xi_1}\right|_{p=p_s} = r - \frac{p_s|z+z_0|}{\tilde{\xi}_1} = 0 , \tag{11}$$

where a tilde above any quantity indicates that it is to be evaluated at the saddle point, $p = p_s$. The notation used in Paper 1 has been retained, so that a saddle point in the complex $p-$plane will be denoted as p_s, except if it lies on the real $p-$axis, where the

designation p_0 will be used. Expanding $T(p)$ in a Taylor series in the vicinity of $p = p_s$ has

$$T(p) \approx T(p_s) + \left.\frac{d^2T(p)}{dp^2}\right|_{p=p_s} (p - p_s)^2 + \cdots \tag{12}$$

as $dT(p)/dp\big|_{p=p_s} = 0$ defines the location of the saddle point. Further,

$$\left.\frac{d^2T(p)}{dp^2}\right|_{p=p_s} = T''(p_s) = -\frac{|z + z_0|\, p_1^2}{\xi_1^2}. \tag{13}$$

The definitions $\tau(p_s) = \mathrm{Re}\left[T(p_s)\right]$ and $\kappa(p_s) = \mathrm{Im}\left[T(p_s)\right]$ are introduced, where $\tau(p_s)$ and $\kappa(p_s)$ are the real travel time term and exponential attenuation term, respectively. Thus, $i\omega T(p)$ has a Taylor series expansion of the form

$$i\omega T(p) \approx i\omega\tau(p_s) - \omega\kappa(p_s) + i\omega T''(p)\big|_{p=p_s} (p - p_s)^2 + \cdots \tag{14}$$

In general, the saddle point solution to the integral in equation (9) may be written as (Brekhovskikh, 1980, Marcuvitz and Felsen, 1973)

$$u_z(r, z, \omega) = \left[\frac{-\omega}{4\pi\rho_1\alpha_1^2}\right] \frac{F(\omega)\, PP(p_s)\, p_s^{1/2} e^{i\omega\tau(p_s) - \omega\kappa(p_s)}}{\left(-rT''(p_s)\right)^{1/2}}. \tag{15}$$

The alternate saddle point approximation used in Paper 1 for this specific problem differs from the above as its derivation yields a real-valued saddle point, p_0. It is dealt with quite comprehensively in that work and will not be presented here.

The approximations to the saddle point solution of the above stated problem, which will be used in the numerical experiments mentioned previously, will now be discussed in more detail. The basis for a numerical integration procedure used to establish the numerical accuracy of these approximations is Equation (8).

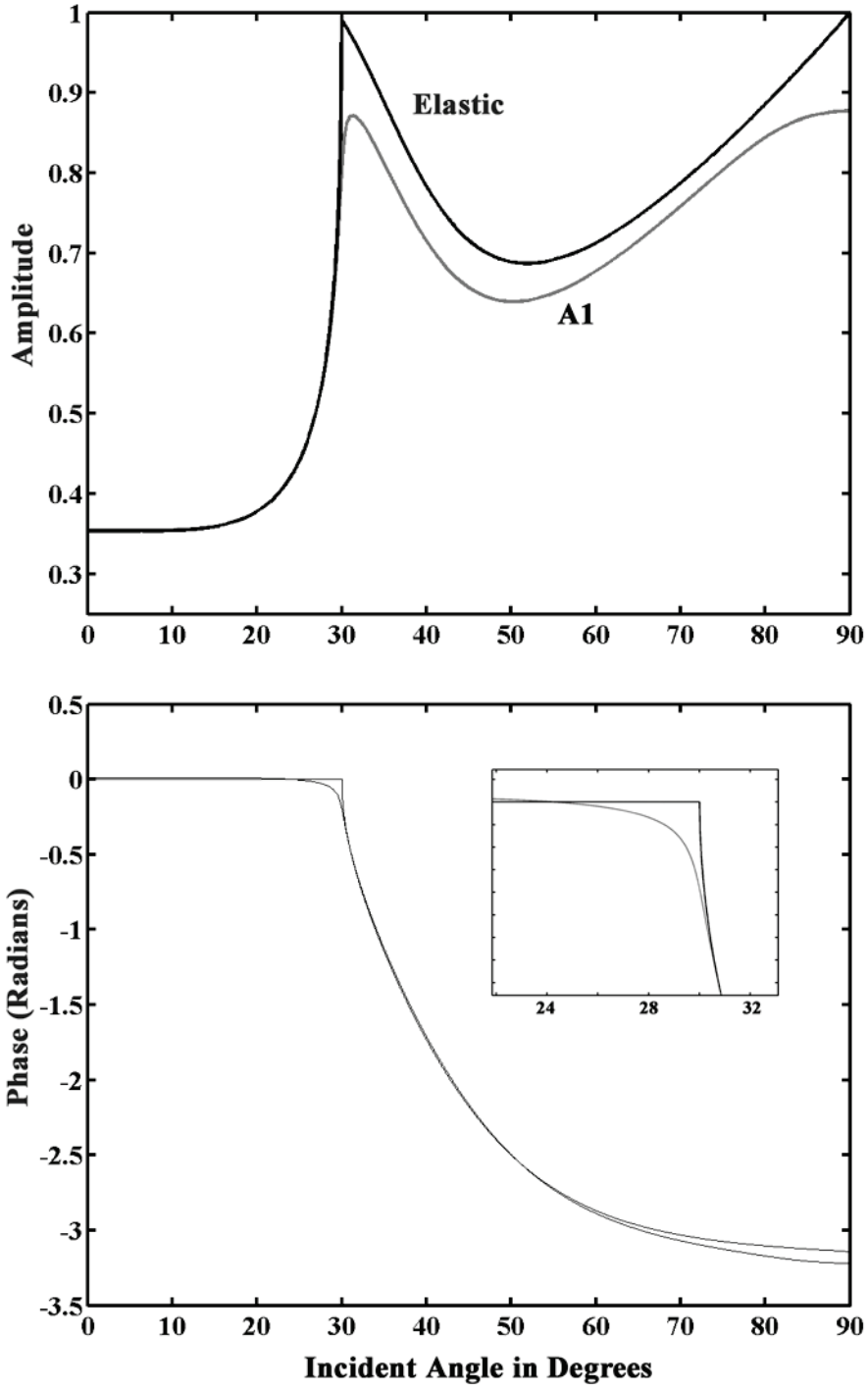

FIG. 1. The PP reflection coefficient at the interface between the two anelastic halfspaces described in Table 1. Approximation 1 $(\mathrm{A1})$ (grey curve) is compared to the elastic case (black curve). Anelasticity is introduced using frequency independent complex velocities.

PP REFLECTION COEFFICIENT

The anomalous saddle point solution dealt with here is for a specific distribution of quality factors in the two anelastic halfspaces: Q_{P_1} and Q_{P_2} with $Q_{P_2} > Q_{P_1}$ (Figure 1). The reflected PP particle displacement in the upper halfspace, where the source and receivers are located, has been a longstanding problem. The motivation here is not to proceed with a rigorous mathematical analysis, but rather to obtain formulae of the geometrical optics type that may be used for the numerical modeling of this anomalous behaviour such that the results are in reasonable agreement with more accurate methods of solution, such as numerical integration. This may require taking some mathematical liberties. However, this will be deemed acceptable if the result is the production of realistic numerical results.

The saddle point approximation discussed in Paper 1 will first be briefly considered. As is standard convention, the derivative of the function $T(p)$, with respect to p, when set equal to zero specifies the saddle point, p_s. $T(p)$, in this first case, is separated into real and imaginary parts. The value of p_0 is obtained from the solution of $d\left\{\mathrm{Re}\left[T(p)\right]\right\}/dp\Big|_{p=p_0} = 0$. As this solution involves only real values, the saddle point is a real valued quantity, located on the real positive axis in the complex $p-$plane. Substituting this value into the imaginary part of the exponential function $T(p)$ produces the attenuation factor expected for wave propagation in an anelastic medium. This modification of the typical saddle point method results in an improved behaviour of the radical $\tilde{\xi}_2 = \left(p_2^2 - p_0^2\right)^{1/2} = \left(\alpha_2^{-2} - p_0^2\right)^{1/2}$ and as a consequence, of the PP reflection coefficient. As indicated earlier, a more detailed analysis of this specific procedure may be found in Paper 1. In what follows this will be referred to as Approximation 1. The plots of the amplitude and phase versus the incident $P-$wave angle for the PP reflection coefficient approximation are shown in Figure 1, together with the elastic case. The parameters of the media are given in Table 1 and are the same as those used in Paper 1. The definition of the manner in which frequency independent (hysteretic) values of Q_j $\left(j = P_1, P_2, S_1, S_2\right)$ are introduced is given in the Introduction. The insert in the phase panel gives a clearer picture of the behaviour of the phase in the vicinity of the elastic case critical point.

From Aki and Richards (1980, 2002) it may be seen that the numerical integration path for this particular problem is along the real $p-$axis $\left(0 < p < \infty\right)$. Assume a closed contour integral in the complex $p-$plane, and neglect the contributions from any poles contained within this closed contour. For a function of p, say $\zeta(p)$, which is analytic at all interior points (except the possible aforementioned poles), within this simple closed contour C, may be written as a consequence of Cauchy's Theorem (Churchill and Brown, 2003) as

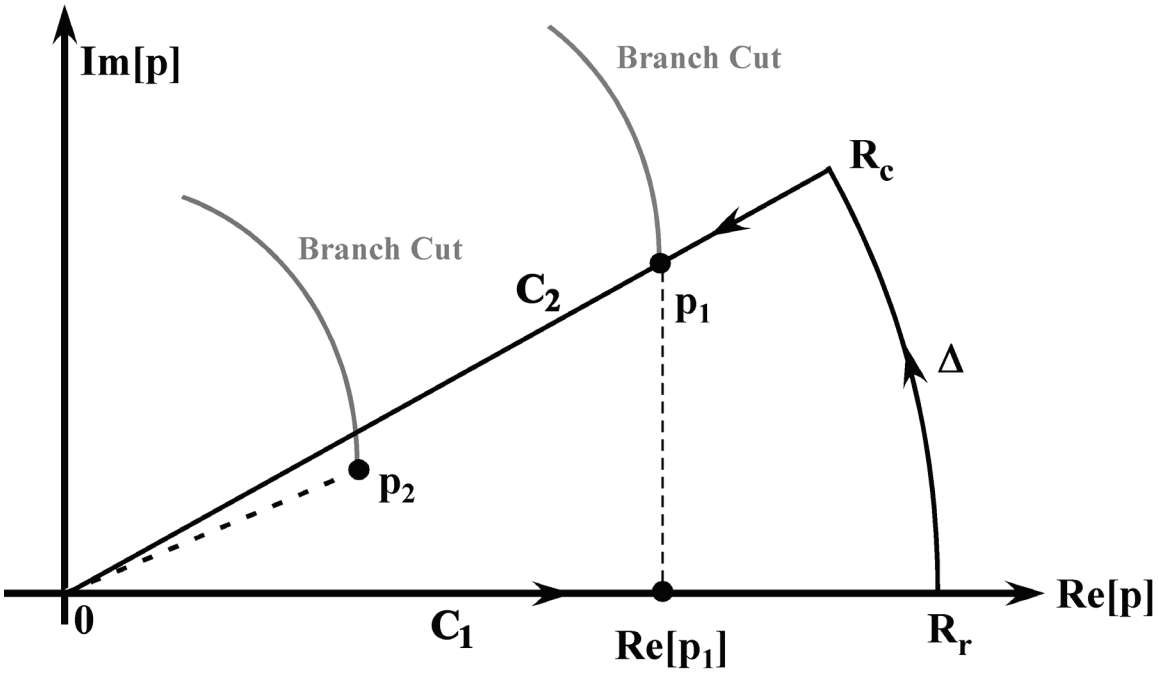

FIG. 2. A schematic of the saddle point and/or numerical integration paths specific to Approximation 2 $(\mathrm{A2})$. The saddle point, p_s, lies on the line connecting the origin with the point p_1. The imaginary axis is scaled significantly with respect to the real axis (black curve). The two numerical integration contours employed are indicated in the figure as C_1 and C_2.

$$\oint_C \zeta(p)\,dp = \int_0^{|R_r|\to\infty} \zeta(p)\,dp + \int_\Delta \zeta(p)\,dp + \int_{|R_c|\to\infty}^0 \zeta(p)\,dp = 0. \qquad (16)$$

Assuming that certain radiation conditions are satisfied for $\zeta(p)$, such that it tends to zero as $|R| \to \infty$, $\int_\Delta \zeta(p)\,dp \equiv 0$, leaving (Figure 2)

$$\int_0^{|R_r|\to\infty} \zeta(p)\,dp = \int_0^{|R_c|\to\infty} \zeta(p)\,dp. \qquad (17)$$

The above equation shows that the numerical integration along the two paths produces identical results. That part of the contour related to the integration along the real $p-$axis will be denoted as C_1, while the other contour in equation (17) will be labelled C_2. It is known from earlier work that the saddle point solution for this problem is constrained to lie on the line joining the origin and the point $p = \alpha_1^{-1} = p_1$, where α_1^{-1} and p_1 were

previously defined. That the "correct" saddle point path lies along this path cannot be assumed from equation (17) because the saddle point is in the vicinity of a branch point along at least part of this path. However, a discrepancy of the type observed in earlier numerical results related to this problem would indicate some additional problem.

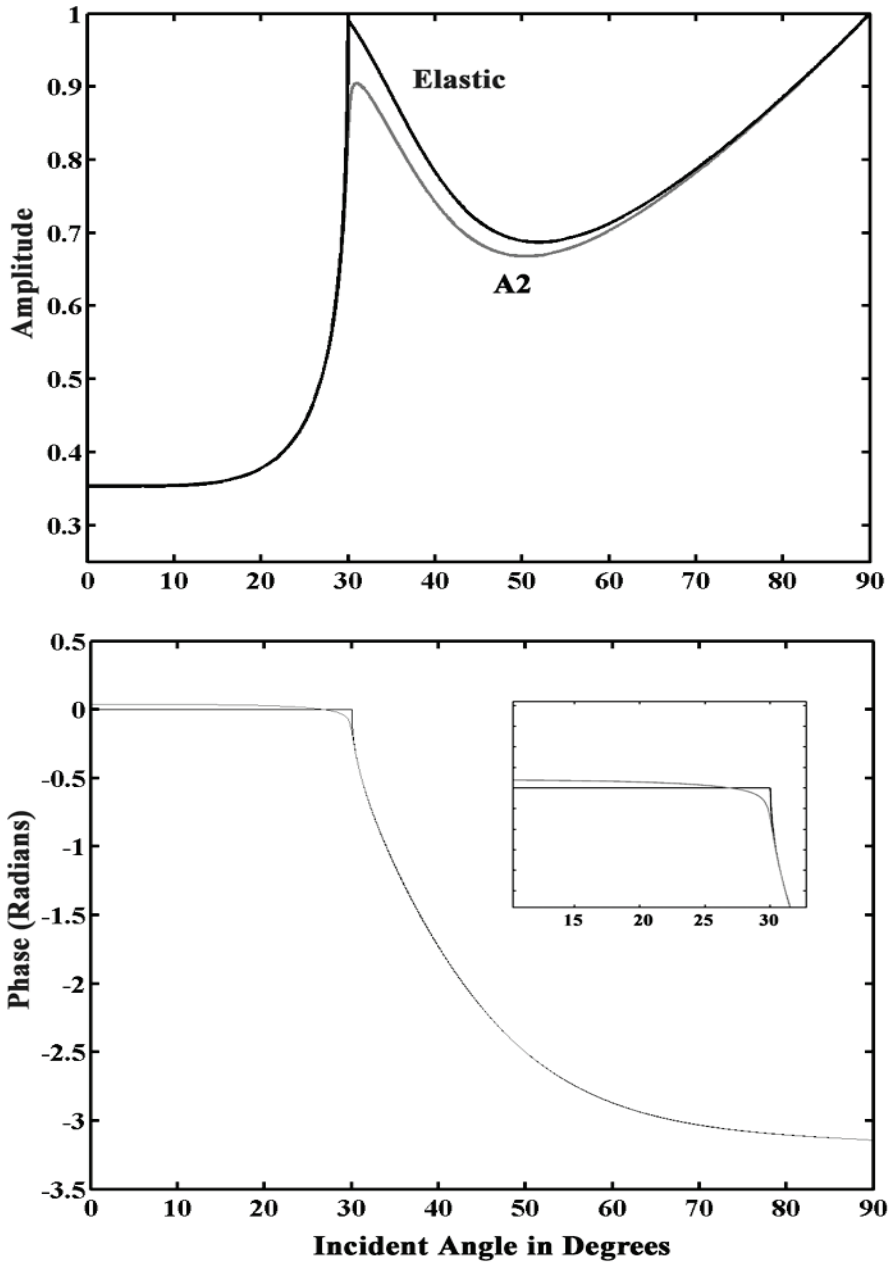

FIG. 3. The PP reflection coefficient at the interface between the two anelastic halfspaces described in Table 1. Approximation 2 $(\mathrm{A2})$ (grey curve) is compared to the elastic case (black curve). Anelasticity is introduced using frequency independent complex velocities.

It was suggested and demonstrated by graphing the PP reflection coefficient in Paper 1 that "forcing" the radical $\tilde{\xi}_2 = \left(p_2^2 - p_s^2\right)^{1/2}$, in the PP reflection coefficient, to take on its complex conjugate value for all values of p_s along the saddle point line in the complex $p-$plane produces good numerical results.. This will be referred to as Approximation 2. The plots of the amplitude and phase versus the $P-$wave incident angle of the PP reflection coefficient for this approximation as well as the elastic case are presented in Figure 3. An insert in the phase panel provides a clearer picture of the behaviour of the phase in the vicinity of the elastic critical point. The values for the media parameters used in the computations are the same used in the Approximation 1 case above.

Before considering the saddle point synthetic trace results related to these two approximations the equality of the two numerical integration contours should be addressed. The model used has both the source, and receiver line located at a distance $z = -1000m$ above the interface between the two anelastic halfspaces. If the elastic case is taken as an guide, the critical distance is at an offset of about $1155m$. The total offset range considered is from $r = 0m$ to $r = 1200m$ with the horizontal distance between two adjacent receivers being $40m$.

In theory, integration along the real $p-$axis $\left(C_1\right)$ is equal to the integration along the line from the origin of the $p-$plane to the point $p = p_1$ $\left(C_2\right)$. However in practice, the two integrations are equal *only if* the complex conjugate of the quantity ξ_2 is used along the second integration path $\left(C_2\right)$ from $p = 0$ to $p = p_1$. If this is not done, the critically refracted (head) wave displays unphysical properties in that it propagates backwards in space and time with apparently incorrect amplitude. This behaviour is shown in panel (a) of Figure 4. Panel (b) shows the correct result if it assumed that the integration along the real $p-$axis $\left(C_1\right)$ is the indicator of correct results. It may be inferred from this that "forcing" the radical ξ_2 to display the same behaviour in the PP reflection coefficient and in any subsequent zero saddle point computations is justified, if only from a numerical perspective.

In computing the synthetic traces by the numerical integration method the velocities are assumed to be frequency dependent. This dependence is established in the fashion described by Futterman (1962) and is discussed in detail in Aki and Richards (1980, 2002). The introduction of an additional parameter for each halfspace, a reference

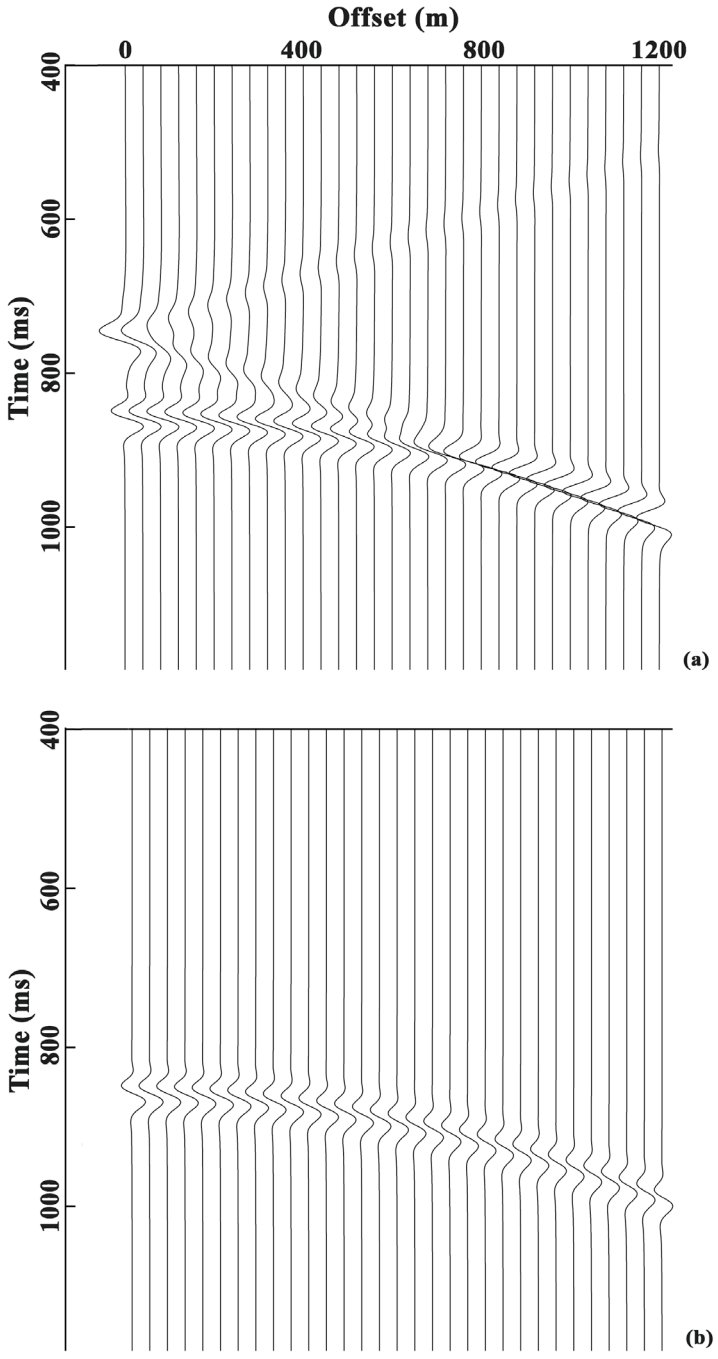

FIG. 4. Integration along C_2 in the complex $p-\text{plane}$. Panel (a) shows the erroneous results obtained if the constraint that ξ_2 is not replaced by its complex conjugate in the integration process. In panel (b), the "correct" synthetic numerical integration traces are displayed. If the results from integrating along C_1 were overlaid in panel (b), the match would be almost exact.

frequency, f_0, of the Gabor[2] source wavelet - $f_R = f_0 = 30Hz$. The relevant formulae at some other circular frequency, ω, in terms of $\omega_R = 2\pi f_R$ of the real values $Q(\omega)$ and $V(\omega)$ and complex value velocity $v(\omega)$ are determined by the sequence of relations

$$Q(\omega) = Q(\omega_R)\left[1 - \frac{1}{\pi Q(\omega_R)} \ln\left(\frac{\omega}{\omega_R}\right)\right] \tag{18}$$

so that

$$V(\omega) = V(\omega_R)\frac{Q(\omega_R)}{Q(\omega)}. \tag{19}$$

which results in

$$\frac{1}{v(\omega)} = \frac{1}{V(\omega)}\left[1 + \frac{i}{2Q(\omega)}\right] \quad (v = \alpha \text{ or } \beta). \tag{20}$$

Equations (18)-(20) correspond to those which appear in Zahradník et al. (2002).

In the next section zero order saddle point synthetic traces will be compared with those obtained from numerical integration for the anelastic model discussed above.

ZERO ORDER SADDLE POINT APPROXIMATIONS

Synthetic traces computed using the two approximate zero order saddle point methods described above are shown next. The model used is as described for the numerical integration synthetic traces. The first offset is at $r = 0$ with 30 further receivers placed at $40m$ intervals so that the maximum offset is $1200m$. If the elastic parameters are used the critical distance is $1155m$ which lies at about trace 29 in the common shot gather of 31 traces. The post-critical offsets were included to see how the saddle point approximations behave without the inclusion of the critically refracted $P_1P_2P_1$ (head) wave (Červený and Ravindra, 1971) or any modification of the saddle point approach to accommodate the range of offsets where a higher order approximation should be used to compensate for a saddle point in the vicinity of a branch point (Marcuvitz and Felsen, 1973, and Červený and Ravindra, 1971, as examples).

As mentioned earlier, a Gabor wavelet is used with a predominant frequency $f_0 = 30Hz$ and a dimensionless damping factor $\gamma = 4$. The time sampling rate is $1ms$ in all traces. The manner of introducing a frequency dependent Q into the saddle point computations is the same as that used for the numerical integration traces described in the previous section.

[2] Gabor wavelet: $f(t) = \sin(2\pi f_0 t)\exp\left[-(2\pi f_0 t/\gamma)^2\right]$ where γ is a dimensionless damping that controls the amplitude spectrum width in the frequency domain and the side lobes of the wavelet in the time domain.

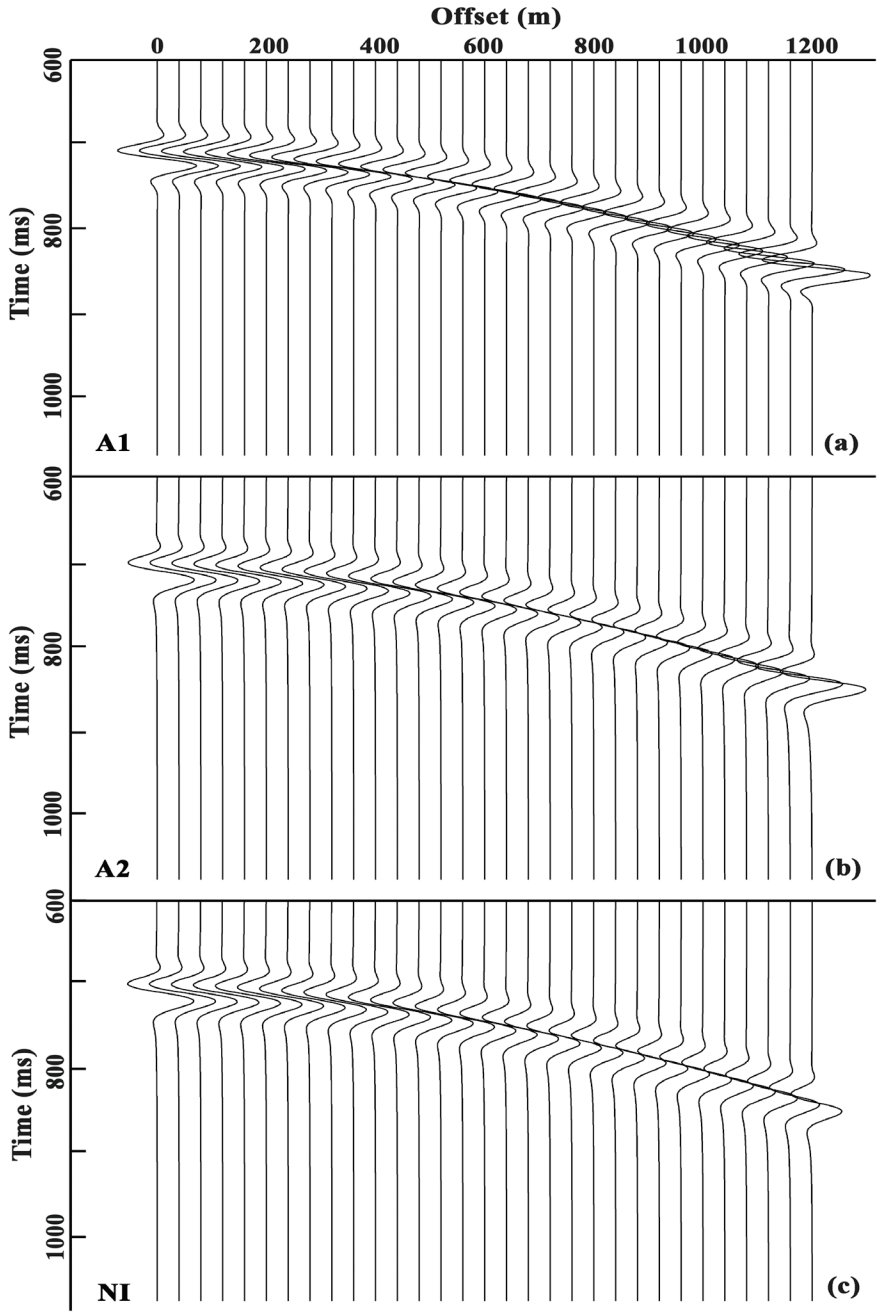

FIG. 5. The two saddle point approximations, $\mathrm{A1}$ and $\mathrm{A2}$, discussed in the text plotted together the numerical integration, NI,solution of the vertical component of reflected PP particle displacement due to $P-\mathrm{wave}$ incidence on an interface separating two anelastic halfspaces. Each of the gathers consists of 31 receivers spaced at $40m$ intervals for an offset range of $\left(0m \le r \le 1200m\right)$.A $30Hz$ Gabor wavelet was used and the time sampling rate is $1ms$. displacement for $P-\mathrm{wave}$ incidence at a plane interface between two anelastic halfspaces. Zero time on the traces corresponds to an actual time of $601ms$. Each of the traces are $500ms$

The three panels in Figure (5) show the 2 saddle point approximations together with the numerical integration result for the model described above and in Table 1. To preserve space, only 500 time points of the traces were plotted, starting at $601ms$ which was assigned as the zero tie point in all of the traces in this figure. The two saddle point approximations are indicated in Figure (5) by $A1$ and $A2$ and numerical integration traces by NI.

In the three panels in Figure (6) the two approximations and the numerical integration traces are compared by plotting all three on a single axis for the offsets $r = 0, 600, \text{and } 1200m$. The line types used in the plotting of the three different traces are defined in the figure caption. The fit between all approximate traces with the numerical integration traces is quite evident, except at $r = 1200m$, which is in the range of offsets for which the reflected and critically refracted arrivals interfere. This is known as the "interference zone". More on this topic may be found in Červený and Ravindra (1971).

After viewing the panels in Figures (6) it becomes evident, that at least in the high frequency or geometrical optics solution, the two saddle point approximations produce consistent results, with approximation 2 producing the best fit with the numerical integration traces. This is to be expected, as A1 incorporates more approximations to produce synthetic results.

CONCLUSIONS

A comparison of saddle point approximations for the case of PP reflection due to incidence of a $P-\text{wave}$, emanating from a point source, at an interface separating two anelastic media has been presented. The two zero order saddle point approximations considered provide numerically proper approaches of dealing with the anomalous amplitude behaviour, observed in problems of this type due to a specific distribution of Q_P values in the two halfspaces. Acceptable results, when compared to the "exact" solution, obtained from a numerical integration algorithm were realized. This comparison of results was done within a numerical context and it may be concluded that if the PP reflection coefficient displays appropriate behaviour, so too will the associated saddle point approximation. Further investigation is still required to determine a proper theoretical explanation for the anomalous behaviour observed.

The first of these approximations, because of its minimized memory requirements and computational speed is in the process of being implemented in a plane layered structure with an arbitrary number of layers and receivers. This is being done for both amplitude versus offset, (AVO), and vertical seismic profile, (VSP), modeling applications.

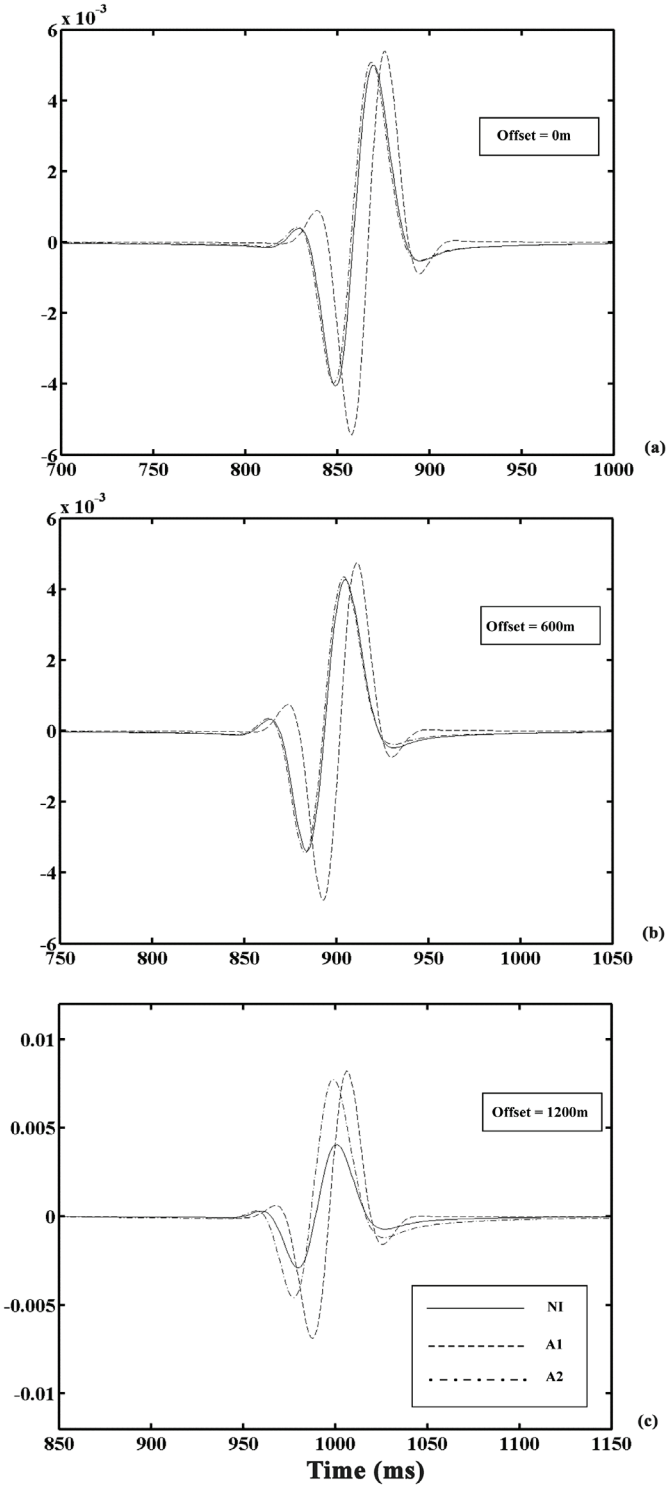

FIG. 6. A comparison of traces at selected offsets of $r = 0, 600$ and $1200m$. Synthetic traces obtained using the two saddle point approximations, $\mathrm{A1}$ and $\mathrm{A2}$, and the numerical integration, NI, approach are plotted on a single time axis. The code identifying each trace type is given in the insert in panel.

REFERENCES

Abramowitz M. and Stegun I.A., 1980. *Handbook of Mathematical Functions,* Dover, New York, NY.

Azimi Sh. A., Kalinin A.V., Kalinin V.V. and Pivovarov B.L., 1968. Impulse and transient characteristics of media with linear and quadratic absorption laws, *Izv. Phys. Solid Earth*, **2**, 88-93.

Aki K. and Richards P.G., 1980. *Quantitative Seismology*, W.H. Freeman and Company, San Francisco, CA.

Aki K. and Richards P.G., 2002. *Quantitative Seismology*, 2nd edition, University Science Books, Saulsalito, CA.

Červený V. and Ravindra, R., 1971. *Theory of seismic head waves*, University of Toronto Press, Toronto.

Churchill, R.V. and Brown, J.W., 2003. *Complex variables and applications*, McGraw-Hill, New York, NY.

Futterman W.I., 1962. Dispersive body waves, *J. Geophys. Res*., **67**, 5279-5291.

Krebes E.S. and Daley, P.F., 2007. Difficulties with computing anelastic plane wave reflection and transmission coefficients, *Geophys. J. Int.*, **16**, 41-55.

Marcuvitz N. and Felsen L.B., 1973. *Radiation and scattering of waves*, Prentice Hall, New Jersey.

Rudd, B.O., 2005. Ambiguous reflection coefficients for anelastic media, *Sixth Workshop Meeting on Seismic Waves in Laterally Inhomogeneous Media,* Geophysical Institute, Academy of Sciences of the Czech Republic and Department of Geophysics, Charles University.(available online at http:/www.ig.cas.cz/activities/Posters/poster.php).

Zahradník J., Jech J. and Moczo P., 2002. Approximate absorption corrections for complete SH seismograms, *Stud. Geophys. Geod*., Special Issue 2002, 133-146.

$\rho\left(\mathbf{g/cm^2}\right)$	$\mathbf{V_{HP}}\left(\mathbf{m/s}\right)$	$\mathbf{V_{HS}}\left(\mathbf{km/s}\right)$	$\mathbf{Q_P}$	$\mathbf{Q_S}$	$\mathbf{f_R}\left(\mathbf{Hz}\right)$
2.1	2500	1000	25	15	30
2.2	5000	2000	40	20	30

Table 1. Parameters of the anelastic two halfspace model used in producing the numerical results presented. These real quantities are used to specify either a constant Q type structure or with the additional of the halfspace reference frequencies, f_R, an anelastic model that is frequency dependent.